Hindawi
Advances in Multimedia
Volume 2022, Article ID 8998225, 12 pages
https://doi.org/10.1155/2022/8998225

Research Article

Building Information Protection Method of Urban Historical Features Based on BIM Technology

Lin Chen,[1] **Xiaolong Chen**,[1] **and Lingyun Lang**[2]

[1]*International School of Design, Sanya University, Sanya 572022, China*
[2]*College of Civil Engineering, Zhengzhou University of Technology, Zhengzhou 450002, China*

Correspondence should be addressed to Lin Chen; linchen@sanyau.edu.cn

Received 22 April 2022; Accepted 26 May 2022; Published 11 June 2022

Academic Editor: Qiangyi Li

In order to improve the building information protection method of urban historical features, this paper combines BIM technology to study the building information protection method of urban historical features and studies the least-squares fitting technology of NURBS curves. On this basis, this paper proposes a fitting method of the constrained least-squares method. Moreover, this paper designs a constrained least-squares method for the requirement of fitting accuracy and gives a method for setting the initial value. In addition, this paper proposes a NURBS interpolation method based on arc length parameter compensation technology. The experimental study verifies that the building information protection method of urban historical features based on BIM technology has a good effect and can effectively promote the building information protection of urban historical features.

1. Introduction

The spatial environment of urban architectural cultural heritage is an important carrier of its ontology, and it also fully nourishes the urban architectural cultural heritage itself. In the long history of China, the architectural space environment has been created with strong traditional cultural characteristics and philosophical concepts. Among them, space is the "qi" of the building, and the building has become the "section" of the space, and they are interdependent and complementary to each other. At the same time, the integration of space environment and architecture has formed the philosophical concept of "Tao follows nature" from nature to nature. The existence of people requires "Qi," and the preservation and continuation of a building also require its own "Qi," which is the infinite bearing and full nourishment of the space environment for the building itself. In such a state of coexistence, the spatial environment of urban architectural cultural heritage also gathers important historical and cultural information.

A city can be regarded as a collection of all the building units that make up the city, so all the individual buildings that make up the city as a whole, regardless of their type, can be called urban buildings [1]. Literature [2] divides urban buildings into variable housing and immutable monuments. The former can last for centuries in the form of residential areas from a collective perspective but is in constant change from a single perspective, while the monument is an invariable factor in the city, a single building, or a group of buildings that have been continuously preserved. Urban buildings that can become monuments generally have relatively important aesthetic and historical value and have the symbolic significance of the city or block, so they have become a constant factor in the city, "reflecting the history of the city, the city's history, the energy of art, being and memory" [3]. The protection of the aesthetics and historical and cultural values of these enduring monuments in cities has long been the consensus of all walks of life in contemporary society. Although there are still different understandings and inclinations in terms of specific protection methods and concepts, the effect of each protection case is pros and cons. There are also many disputes, but with the conclusion of various protection conventions and charters, the concept of protection has been deeply rooted in the hearts of the people, and most urban monuments have been more or less protected and respected [4]. Compared with the

enduring monuments, the ordinary urban buildings that constitute the vast majority of the urban architectural body, the "housing" in Rossi's words, are in a state of constant change in the process of urban development. The renewal and development of urban buildings are also a reflection of the vitality of the city and the materialized embodiment of the economic development of the city [5]. Whenever the urban economy is booming or the urbanization movement is advancing vigorously, the scope and degree of renewal and change of urban buildings will be greatly expanded and strengthened. The mix and collage of old and new buildings from different eras reflect the history and context of urban development and are also a materialized carrier of urban time and memory. Although those "eternal" monuments are more distinctive and symbolic, the overall style and impression of the city are composed of monuments and a large number of common urban buildings, and compared to those "eternal" in terms of monuments that remain unchanged for a long time, the ordinary urban buildings that have been changing and updating can reflect the vitality of urban development and prosperity and are the most accurate and true materialization of urban character traits and social life [6]. However, judging from the current situation of the rapid urbanization movement in our country, the research and understanding of the historical value of these ordinary urban buildings seem to be still in a conceptual gap.

The historical value of an urban building lies in the historical information it carries and conveys, and the temporal element is the material carrier for carrying and conveying this information [7]. In general, the temporal elements of urban buildings can be divided into two categories. One is the elements that are present at the beginning of its construction, such as the architectural form, style, structure, material, and decoration of the building when it is built [8]; these elements reflect the social economy, culture, technology, aesthetics, and other aspects of information when the building is built. The other type is the elements that gradually increase in the years after its completion, such as changes in the maintenance, repair, addition or demolition, modification, and other behaviors of the building in the future, in addition to the impact of the natural environment on the building, such as Erosion and weathering of materials, attachment of plants, and traces of animal life [9]. For the former type of elements, we can call them native elements, while the latter can be called additive elements. For the protection of the historical value of urban buildings, the specific action is to protect these temporal elements, but there are always different opinions on which temporal elements are more in the position of limited protection [10]. For the protection and restoration of historical buildings, the current two main schools are based on different understandings of the above two types of temporal elements. Literature [11] believes that "restoration in a sense is to restore the originality of the original style of the building, for which all subsequent additions must be removed." There is something that has never existed in the original. And the authenticity restoration also pays enough attention to the superimposed time element. Literature [12] put forward the idea of "documentary restoration," relying on critical stylistic restoration. A falsification of art is a trap left to future generations. It advocates the principle of identifiability of newly repaired parts, and the repaired and added parts should be clearly distinguished from the old body in terms of materials and methods, so as to protect the historical authenticity of the heritage. It can be said that Poyeo's proposition has created a road of authenticity and restoration in the protection of historical buildings.

In the work of historical building protection, massive image analysis and data management will be involved from the preliminary status survey, design stage, construction stage, and later supervision and maintenance process, and each historical building is an independent individual. To conduct comparative research on them, we extract their characteristics and commonalities to provide certain decision support for the study of the urban context, which all involve the timely and accurate acquisition and analysis of massive data. In recent years, the analysis and collection of massive visual data have become one of the research directions of BIM [13]. At the same time, the management of historical building protection business needs to be supported by many information resource databases, such as historical building original database, historical building maintenance information database, historical building maintenance engineering method database, historical building knowledge database, historical building material knowledge database, and historical building job responsibilities knowledge [14]. How to collect, store, and extract these single and fragmented historical data is necessary to collect data quickly and effectively and integrate it into the building information model and integrate it into the system database. The knowledge base of historical buildings not only has a large amount of data but also changes rapidly with the passage of time and technological innovation, and a tracking and monitoring mechanism needs to be established [15].

The visual display of historical buildings is mainly to construct three-dimensional models of building components according to the real size of historical buildings. By entering the integrated information of component parameters in BIM, combined with the relevant data collected in the monitoring and management of pests and diseases, it is possible to realize the comprehensive data body of building information with the static building model of the historical building as the spatial reference and the dynamic monitoring pest information as the linkage display object and then realize the visualization of early building 3D model scene, the visualization of building diseases and insect pests, and the visualization of building health status [16]. The 3D visualization of historical buildings mainly collects the real 3D data of historical buildings, realizes the fast and convenient real 3D digitization of historical buildings, and can be browsed and displayed through the mobile terminal. The most important part of the visualization of 3D real scenes is to realize the visualization of the mobile terminal display system. For example, basic functions such as browsing, zooming in, and zooming out of historical buildings can be performed in the mobile terminal, and certain interactive data query and analysis functions can be assisted, which can provide a variety of roaming methods to meet the needs of

different users [17]. The visualization of pests and diseases in historical buildings is based on the collection and entry of monitoring data of pests and diseases and presents the health status of buildings in real time and dynamically. These contents can include the entry, modification, and deletion of the attribute data and picture data of the information points of pests and diseases, the visualization of the 3D scene of the monitoring information of the pests and diseases of the ancient buildings, the query of the information points of the pests and diseases, the statistics of the distribution of the pests and diseases, and the export of the query information of the disaster points, etc. [18].

This paper combines BIM technology to study the method of building information protection of urban historical features and constructs an intelligent method to improve the effectiveness of building information protection of urban historical features.

2. Building Structure Curve Algorithm

2.1. Linear Interpolation. The interpolation of the parameter curve is mainly divided into the following three categories: speed control interpolation, uniform interpolation, and interpolation that automatically adjusts the feed speed. The parameter increment of uniform interpolation is a constant, which cannot automatically adjust the speed change, and is generally not used for parameter curve interpolation. The interpolation that automatically adjusts the feed speed is actually proposed on the basis of uniform interpolation. The speed and time are functional relationships, and the algorithm is the same as that of uniform interpolation. Currently, the most commonly used is nonuniform rational B-spline interpolation. Using the first-order approximation of the Taylor expansion method can realize the uniform change of the feed rate, and the second-order approximation of the Taylor expansion method can realize the smooth transition of the feed rate and reduce the speed fluctuation. However, these algorithms only consider the problem of interpolation feed speed control and do not consider the accuracy of interpolation processing parts.

Figure 1 shows the overall structure of the NURBS interpolation algorithm. The first is the processing of interpolation speed, which is divided into real-time interpolation processing and non-real-time interpolation processing. The traditional interpolation processing usually adopts interpolation preprocessing, and a large number of straight line segments or arc segments approximate the curve. The data information of these straight line segments or arc segments is read into the interpolation memory, and the planning of the velocity between the solution point segments and the planning of the acceleration at the transition point is processed. This approach is often referred to as the look-ahead approach. The NURBS interpolation process is more complicated, and it is difficult to calculate it in real time during the interpolation process. Most of the current research methods are offline preprocessing before the interpolation process. The main research contents of interpolation preprocessing are speed processing planning of NURBS curve interpolation, detection of speed-sensitive areas, acceleration control planning at curvature changes, and speed processing at speed transition points.

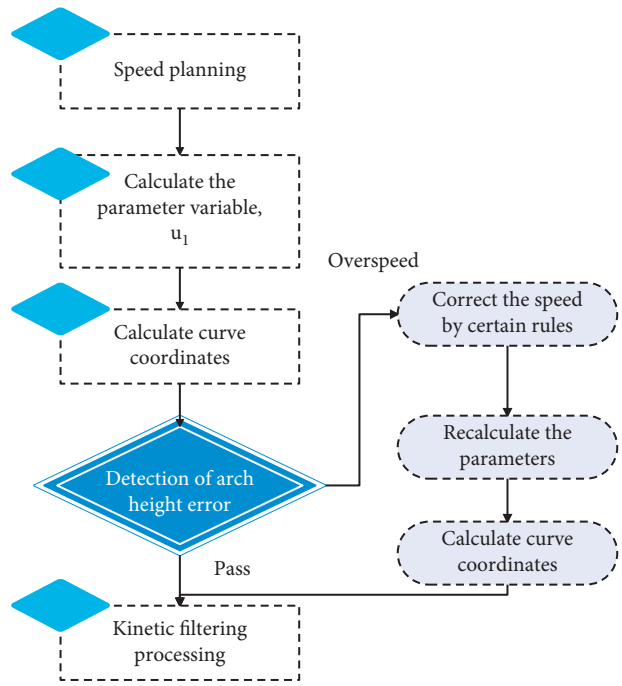

Figure 1: Structure diagram of NURBS interpolation algorithm.

2.2. The Principle of Direct Interpolation of NURBS Curve. A NURBS is completely defined by four parameters: weight factor, control vertex, node vector, and basis function. These four parameters are the key to the commands of the building's intelligent structure drawing system. The building intelligent structure drawing system performs real-time calculations to generate the NURBS curve and drives the machine tool according to the preset feed speed to process the shape of the NURBS curve and surface.

We assume that the parametric equation of a NURBS curve is

$$C(u) = [x(u)y(u)z(u)]. \tag{1}$$

The time function u is the curve parameter, denoted as $u(t_i) = u_i, u(t_{i+1}) = u_{i+1}$. By Taylor expansion of the parameter u with respect to time t, the first-order approximate expression can be obtained:

$$u_{i+1} = u_i + \frac{du}{dt}\Big|_{t=t_i}(t_{i+1} - t_i). \tag{2}$$

$T = t_{i+1} - t_i, T$ is the interpolation period.

The second-order approximate expression for the parameter u is

$$u_{i+1} = u_i + \frac{du}{dt}\Big|_{t=t_i}(t_{i+1} - t_i) + \frac{1}{2}\frac{d^2u}{dt^2}\Big|_{t=t_i}(t_{i+1} - t_i)^2. \tag{3}$$

The contour errors of the first-order and second-order approximate recurrences are basically equal. If the instantaneous velocity at the curve interpolation point is $v\prime(t)$, then,

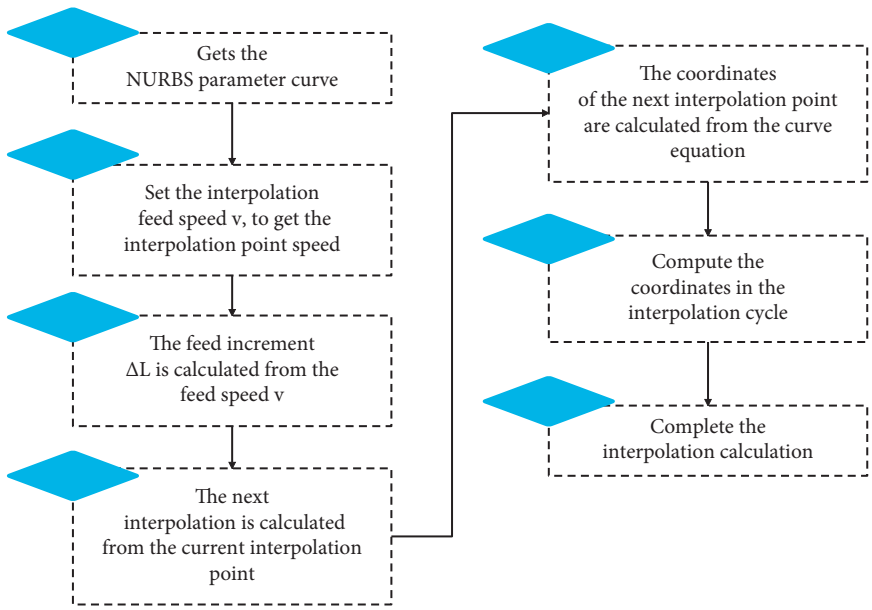

Figure 2: Flow chart of NURBS curve interpolation.

$$v'(t) = \frac{ds}{dt} = \frac{ds}{du}\frac{du}{dt},$$
$$\frac{du}{dt} = \frac{v'(t)}{ds/du}. \tag{4}$$

Usually, the curve speed $v'(t)$ is not the machining feed speed b, because the machining feed speed is the ratio of the tiny straight line segment to the feed time, and the curve feed speed is the ratio of the arc length of the tiny curve segment to the feed time. Because the feed time during interpolation is relatively short, it is approximately considered that the microcurve segment is equal to the microstraightness; that is, the curve speed $v'(t)$ is equal to the machining feed speed $v(t)$.

Among them,

$$\frac{ds}{du} = \sqrt{\left(x'^2\right) + \left(y'^2\right) + z\prime},$$
$$x = p_x(u) y = p_y(u) z = p_z(u), \tag{5}$$
$$x\prime = \frac{dp_x(u)}{du} y' = \frac{dp_y(u)}{du} z' = \frac{dp_z(u)}{du}.$$

From the above formula, $du/dt = v(t)/\sqrt{(x')^2 + (y')^2 + (z')^2}$ can be deduced.

The first-order approximate expression $u_{i+1} = u_i + Tv(t)/\sqrt{(x')^2 + (y')^2 + (z')^2}$ can be obtained.

In the interpolation process, the next interpolation point position C_{i+1} can be obtained by substituting u_{i+1} into the NURBS curve equation. Obviously, this calculation will cause a certain bow height error, that is, the normal distance between the fitted straight line segment and the curved arc.

2.3. NURBS Curve Interpolation Process. The flowchart of NURBS curve interpolation is shown in Figure 2.

3. NURBS Curve Fitting Technique

Compared with Bezier curves and B-spline curves, NURBS curves can express complex free-form surfaces more flexibly and accurately and are uniquely determined by the International Organization for Standardization (ISO) as the expression form of free-form surfaces and geometric products. Moreover, it has been successfully applied in the field of CAD/CAM/CNC.

Compared with Bezier curves and B-spline curves, NURBS curves can express complex free-form surfaces more flexibly and accurately and are uniquely determined by the International Organization for Standardization (ISO) as the expression form of free-form surfaces and geometric products. Moreover, it has been successfully applied in the field of CAD/CAM/CNC. The vertical distance obtained by projecting the building information point Q_i onto the curve is called the approximation error e_i. It is stipulated that the approximation error e_i of each building information point cannot be greater than the maximum error limit E, and the curve is required to pass through Q_0 and Q_m. Therefore, it can be concluded from the conditions of the above two fitting methods that the fitting method is generally used.

3.1. Least Squares Fitting. The least-squares fitting of the NURBS curve is performed on the coordinate positions of discrete building information points, and the trajectory path of the building is generated by fitting. In the fitting process, the fitted NURBS curve data information and error limit E should be input at the same time. In order to avoid nonlinear problems, we generally take the weight factor $\omega = 1$, assume $P \geq 1, n \geq P$, give $Q_0 \cdots\cdots Q_m$, and try to find a P-th NURBS curve:

$$C(u) = \sum_{i=0}^{n} N_{i,p}(u) P_i \quad u \in [0]. \tag{6}$$

Practice shows that chord length parameterization can usually achieve ideal results. When a set of building structure data point sequences $Q_i \quad (i = 0, 1, 2, \ldots, m)$ is known, its chord length parameterization is as follows.

The total chord length is

$$L = \sum_{i=1}^{k} \left| Q_i - Q_{i-1} \right|,$$
$$\overline{u}_k = \overline{u}_{k-1} + \frac{\left| Q_k - Q_{k-1} \right|}{\sum_{k-1}^{n} \left| Q_k - Q_{k-1} \right|}, \quad k = 1, 2, \ldots m - 1. \tag{7}$$

Then, $\overline{u}_0 = 0; \overline{u}_n = 1$.

We set the node vector $U = \{u_0, \cdots, u_r\}$ and the parameter value $\{\overline{u}_k\}$ of each data point, and the configuration of the node should be distributed according to the parameter value $\{\overline{u}_k\}$. If c is a positive real number, $i = \operatorname{int}(d)$ represents the largest integer equal to or less than c. A total of $n + q + 2$ nodes are needed, so there are n-q inner nodes and $n - q + 1$ inner node intervals. Some researchers have proposed the following methods to determine inner nodes:

$$c = \frac{m + 1}{n - q + 1}. \tag{8}$$

The inner node of the domain is $i = \operatorname{int}(jc), \alpha = jc - i$:

$$u_{q+j} = (1 - \alpha)\overline{u}_{i-1} + \alpha \overline{u}_i, \quad j = 1, 2, \ldots, n - q. \tag{9}$$

Formula (9) ensures that each node interval includes at least one $\{\overline{u}_k\}$.

Two conditions for building information point approximation are satisfied:

(1) It is necessary to ensure that the start and end points of the building information points coincide with the spline curve, namely: $C(U_0) = Q_0, C(U_m) = Q_m$;

(2) The remaining data points $Q_i \quad (i = 1, 2, \ldots, m - 1)$ are approximated by the least-squares method; that is, the objective function is

$$f = \sum_{j=1}^{m-1} \left| JQ \begin{pmatrix} \sim \\ - \quad j \\ \\ \end{pmatrix} C \right|, \tag{10}$$

where $D_i (i = 1, 2, \ldots, n - 1)$ is the minimum value of $n - 1$ control vertices, and $\tilde{u}_j (j = 1, 2, \ldots, m)$ is the precomputed parameter value.

In general, a curve approximated by least squares cannot pass exactly through the data point $Q_j \quad (j = 1, 2, \ldots, m - 1)$ and $C(\tilde{u}_j)$ is not the closest point on the curve to the point Q_i. We set

$$\begin{aligned} R_j &= Q_j -_{,0} N(\widetilde{kj}) \forall Q_n, \\ & k(\sim N)m, \\ Q, \ldots, j &= 1. \end{aligned} \tag{11}$$

When the parameter values $\tilde{u}_j$ and (11) are substituted into formula (10), we have

$$f = \sum_{j=1}^{m-1} \left[R_j \cdot R_j - 2 \sum_{i=1}^{n-1} N_i, k(\tilde{u} j)\left(R_j \cdot D_i\right) + \left(\sum_{i=1}^{n-1} N_i, k\left(\tilde{u}_j\right) D_i \right) \cdot \left(\sum_{i=1}^{n-1} N_i, k\left(\tilde{u}_j\right) D_i \right) \right]. \tag{12}$$

When applying standard linear least-squares fitting techniques, to minimize the objective function f, it should make the derivative with respect to $n - 1$ control points $D_i \quad (i = 1, 2, \ldots, n - 1)$ equal to zero. Its first partial derivative is

$$f_{\min} \Rightarrow \frac{\partial f}{\partial D_\ell} = 0, \quad \ell = 0, 1, \ldots, n,$$

$$\frac{\partial f}{\partial D\ \ell} = \sum_{j=1}^{m-1} \left(-2 N_{\ell,k}\left(\tilde{u}_j\right) R_j + 2 N_{\ell,k}\left(\tilde{u}_j\right)_{i=1}^{n-1} N_{i,k}\left(\tilde{u}_j\right) D_i \right),$$

$$\text{That is; } \sum_{i=1}^{n-1} \left(\sum_{j=1}^{m-1} N\ell, k \begin{pmatrix} \sim \\ u \quad j \\ \\ \end{pmatrix}, Ni \begin{pmatrix} \sim \\ u \quad kj \\ \\ \end{pmatrix} \right) \sum_{j=1}^{m-1} \ell, \begin{pmatrix} \sim \\ N \quad k \\ \\ \end{pmatrix}. \tag{13}$$

Formula (11) is a control point, and $D_1, D_2, \ldots, D_{n-1}$ is a linear equation of unknown quantity. If $\ell = 1, 2, \ldots\ m - 1$, then the equation system of $n - 1$ equations containing $n - 1$ unknown quantities is obtained, namely:

$$\left(N^T N\right) D = R. \tag{14}$$

The matrix $(N^T N)$ in formula (12) is positive definite, and the Gaussian elimination method can be used to solve the control points.

Among them, N is the $(m - 1) \times (n - 1)$ scalar matrix.

$$N = \begin{bmatrix} N_{1,k}(\tilde{u}_1) & \cdots & N_{n-1,k}(\tilde{u}_1) \\ \vdots & \ddots & \vdots \\ N_{1,k}(\tilde{u}_{m-1}) & \cdots & N_{n-1,k}(\tilde{u}_{m-1}) \end{bmatrix}. \tag{15}$$

R and D are column vectors of $n - 1$ points.

$$R = \begin{bmatrix} N_{1,k}(\tilde{u}_1) R_1 + \cdots + N_{1,k}(\tilde{u}_{m-1}) R_{m-1} \\ \vdots \\ N_{n-1,k}(\tilde{u}_1) R_1 + \cdots + N_{n-1,k}(\tilde{u}_{m-1}) R_{m-1} \end{bmatrix},$$
$$D = \begin{bmatrix} D_1 \\ \vdots \\ D_{n-1} \end{bmatrix}. \tag{16}$$

3.2. Constrained Least-Squares Fit. The distribution of building information points directly affects the shape of the NURBS curve. If the building information points are closely distributed, it is not conducive to the fitting of the NURBS curve. It is easy to swing and twist at the first and last positions of the fitted NURBS curve. Moreover, evenly distributed building information points are easy to fit into a NURBS curve, and the above problems generally do not occur. Therefore, controlling the start and end points is crucial to the shape of the curve formed by the fit. Sometimes, it is also controlled according to the curvature change at the beginning and end of the curve to ensure a smooth transition at the connection point between the beginning and end of the curve. The constrained fitting problem is basically a constrained minimization problem, and the constraint equation is

$$MD = T, \tag{17}$$

where M is a matrix with $(q+1)\times(n+1)$ elements as scalars, and T is a matrix with $(q+1)\times 3$. An additional unknown λ_k is introduced to solve the constrained least squares problem according to the operation method of the Lagrange multiplier method.

$$A = [\lambda_k], \tag{18}$$

is a vector of Lagrange multipliers; each λ_k has the same dimension as the $\{Q_i\}$ vector. According to the Lagrange multiplier method, the following expressions equation (17) for the unknowns D and A are minimized:

$$\left(S^T - D^T N^T\right)(S - ND) + A^T(MD - T). \tag{19}$$

When we take the derivative of D and A separately and set them to zero, the matrix form of the final solution result is

$$\begin{bmatrix} N^T N & M^T \\ M & 0 \end{bmatrix}\begin{bmatrix} D \\ A \end{bmatrix} = \begin{bmatrix} N^T Q \\ T \end{bmatrix}. \tag{20}$$

We solve the system of equation (20) to get D and A, where the matrices $N^T N$ and $M(N^T N)^{-1}M^T$ are invertible matrices; then,

$$\begin{aligned} A &= \left(M\left(N^T N\right)^{-1} M^T\right)^{-1}\left(M\left(N^T N\right)^{-1} N^T Q - T\right), \\ D &= \left(N^T N\right)^{-1} N^T Q - \left(N^T N\right)^{-1} M^T A. \end{aligned} \tag{21}$$

In order to make the curve fit ideally at the beginning and end points, the derivative values of each order at the beginning and end points are generally equal to those at the beginning and end points of the fitted curve. The first-order derivative constraint is used here. Its essence is the tangent vector at the start and end points, and the derivative value calculated at the start and end points is used as the constraint derivative of the fitting curve. The cut-off at the start point is P_0, and the cut-off at the end point is P_n. If

$$\begin{aligned} \Delta\overline{u}_k &= \overline{u}_k - \overline{u}_{k-1}, \\ q_k &= Q_k - Q_{k-1}, \\ d_k &= \frac{q_k}{\Delta\overline{u}_k}, \\ a_k &= \frac{\Delta\overline{u}_k}{\Delta\overline{u}_k + \Delta\overline{u}_{k+1}}, \end{aligned} \tag{22}$$

then, $\begin{matrix} P_k = (1-a_k)d_k + a_k d_{k+1} \\ P_0 = 2d_1 + P_1, P_n = 2d_n - P_{n-1} \end{matrix}$.

Then, according to the K-th equation of the NURBS curve, the first derivative of the beginning and end points of the curve is obtained as

$$\begin{aligned} C'(0) &= \sum_{i=0}^{n} N'_{i,p}(0)P_i = P_0, \\ C'(1) &= \sum_{i=0}^{n} N'_{i,p}(1)P_i = P_n. \end{aligned} \tag{23}$$

Then, the constraints are

$$\begin{aligned} M &= \begin{bmatrix} N'_0(0) & N'_1(0) & \dots & N'_n & (\uparrow \\ N'_0(1) & N'_1(1) & \dots & N'_n & (\end{bmatrix}, \\ T &= \begin{bmatrix} P_0 \\ P_m \end{bmatrix}. \end{aligned} \tag{24}$$

Finally, the starting and ending control points are obtained according to formula (18), and the remaining control points can be calculated by the least square method.

3.3. Constrained Fit to Specified Accuracy. Generally, $k+1$ (the least here) control points are used at the beginning of the iteration, and an approximation curve is obtained by fitting the building information points with the above derivation. After each fitting, we can check whether the curve deviation is less than E according to the maximum deviation formula until the required approximation error E is met. When the number of building information points is equal to the number of control points, the approximation error $E = 0$. The error check calculation formula is

$$\max_{0\le j\le m}\left(\min_{0\le u\le 1}\left|Q_j - C(u)\right|\right). \tag{25}$$

Control points should be set in advance when calculating building information points, but the distribution of actual building information points is very tight. These building information points should be fitted by the NURBS curve, and the number of control points is relatively large. If these control points are used as initial control points, the computational load will be large. In this paper, the number of initial control points is estimated according to the value of the corner of the building information point.

$$n_{\text{int}} = p + \text{int}\left(\sum_{i=1}^{m}\frac{\theta_i}{90}\right) + 2 \quad i = 1, 2\because m. \tag{26}$$

Among them, $\theta_i = arccQ_{s_1}(Q_iQ_iQ_{1i}\| \quad Q_{1i}\|\Phi_i \quad Q_i \leq i = 1, 2; m$.

The number of initial control points set in this way is more reasonable, which reduces the number of iterations and avoids the instability of any control point.

3.4. Curve Approximation Algorithm. If the distance between the fitted NURBS curve and the building information point exceeds the limit error E, the number of control vertices should be increased to reduce the fitting error. There is a certain relationship between the change in the number of control points and the node vector. In this paper, the node vector is uniformly inserted into the node. Within the defined interval, if the distance between two building information points and the fitted curve exceeds the limit error, a control vertex is added between the two points. Then continue to detect the distance between the building information points and the fitted curve, and stop increasing the number of control points if the distance between the two is within a limited error. In the iterative process, when $n \geq n_{\text{int}}$, the number of control points and node vectors is readjusted for fitting, as shown in Figure 3.

3.5. NURBS Real-Time Interpolation Algorithm. In the process of drawing and processing building intelligent structures, it is necessary to obtain the requirements of high precision of processed parts in the interpolation process. In this paper, the fluctuation of the feed rate and the contour error of the machined part are used as the evaluation criteria. In the NURBS curve interpolation process, the curvature of the curve interpolation point is usually used to calculate the contour error E_i at the parameter u_i (as shown in Figure 4).

Figure 4 is approximated by a segment of arc to represent the NURBS curve in the interval $u \in [u, u_i + 1], \rho_i$ is the radius of curvature at $u = u_i$, and $\rho_i = 1/K_i$. $L = \|C(u_{i+1}) - C(u_i)\|$, the contour error is represented by the interpolation point curvature calculation, and the contour error can be obtained through the geometric relationship as

$$E_i = \rho_i - \sqrt{\rho^2 - \left(\frac{L_i}{2}\right)} = \rho_i - \sqrt{\rho^2 - \left(\frac{V(u_i)T}{2}\right)^2}. \tag{27}$$

Among them, the radius of curvature of the point is calculated as follows:

$$\rho_i = \frac{1}{K_i} = \frac{\|dC(u)/du\|^3_{u=u_i}}{\|dC(u)/du \times d^2C(u)/du^2\|_{u=u_i}}. \tag{28}$$

If the highest contour error required in the machining process is δ, the feed rate under the required error is

$$V(u_i) = 2\sqrt{\frac{\rho_i^2 - (\rho_i - E_{\max})^2}{T}}. \tag{29}$$

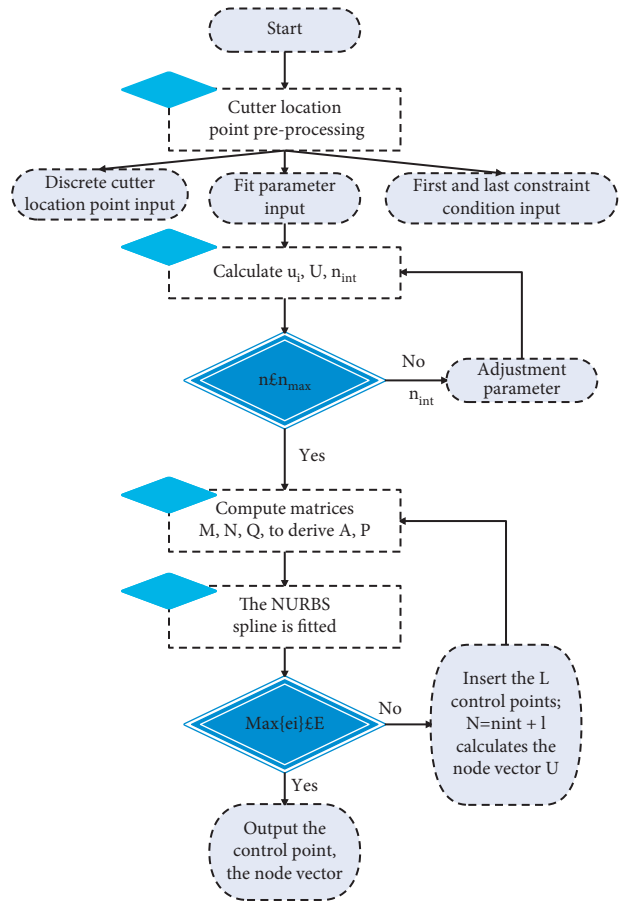

Figure 3: NURBS curve fitting process for constraints.

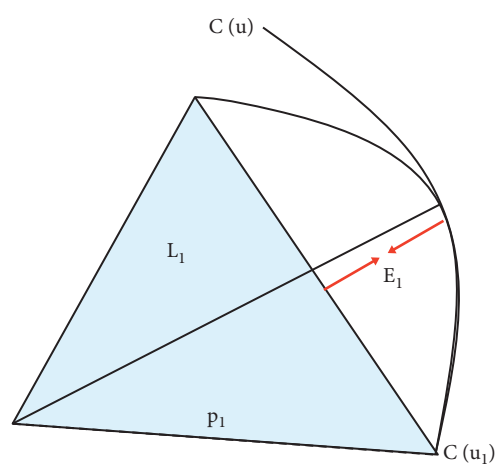

Figure 4: Geometric relationship of error solving.

If E_i satisfies $E_i \leq \delta$, the interpolation calculation process will continue with the interpolation calculation of the next point. If E_i satisfies $E_i > \delta$, the interpolation process will adjust the feed rate $V(u_i)$, return to the current interpolation point, and recalculate the interpolation of the next point at the adjusted feed rate.

The control of acceleration and deceleration in the whole interpolation process directly affects the stability of the

system. By controlling the variation and fluctuation of the speed to the maximum extent, the vibration of the building intelligent structure drawing machine tool is reduced. The process of S-type acceleration and deceleration is divided into 7 different stages: decrease deceleration stage, increase acceleration stage, uniform deceleration stage, uniform acceleration stage, increase deceleration stage, decrease acceleration stage, and uniform speed stage.

Figure 5 shows the arc length, speed, acceleration, and increase acceleration curves of the S-type acceleration and deceleration mode.

The calculation formula of each stage acceleration of typical S-shaped acceleration and deceleration is as follows:

$$a(t) = \begin{cases} Jt, & 0 \le t \le T_1, \\ A, & T_1 \le t \le T_2, \\ A - Jt, & T_2 \le t \le T_3, \\ 0, & T_3 \le t \le T_4, \\ -Jt, & T_4 \le t \le T_5, \\ -A, & T_5 \le t \le T_6, \\ -A + Jt, & T_6 \le t \le T_7. \end{cases} \tag{30}$$

The feed rate can be obtained by integrating a obtained from the above formula:

$$f(t) = \begin{cases} f_s + \frac{1}{2}Jt^2, & 0 \le t \le T_1, \\ f_1 + At, & T_1 \le t \le T_2, \\ f_2 + At - \frac{1}{2}Jt^2, & T_2 \le t \le T_3, \\ f_3, & T_3 \le t \le T_4, \\ f_4 - \frac{1}{2}Jt^2, & T_4 \le t \le T_5, \\ f_5 - At, & T_5 \le t \le T_6, \\ f_6 - At + \frac{1}{2}Jt, & T_6 \le t \le T_7. \end{cases} \tag{31}$$

In the formula, f_s is the initial feed rate.

In this paper, parameter compensation is proposed based on the interpolation point parameters obtained by the Taylor expansion method, so that the compensated parameters can accurately express the arc length coordinates of the NURBS curve. We assume that the spatial parameter curve is $C(u) = [x(u)y(u)z(u)]$, where u is the curve parameter. According to the existing interpolation algorithm of the NURBS curve analyzed above, it can be obtained that the Taylor expansion method approximates the first order, and the second-order expression is

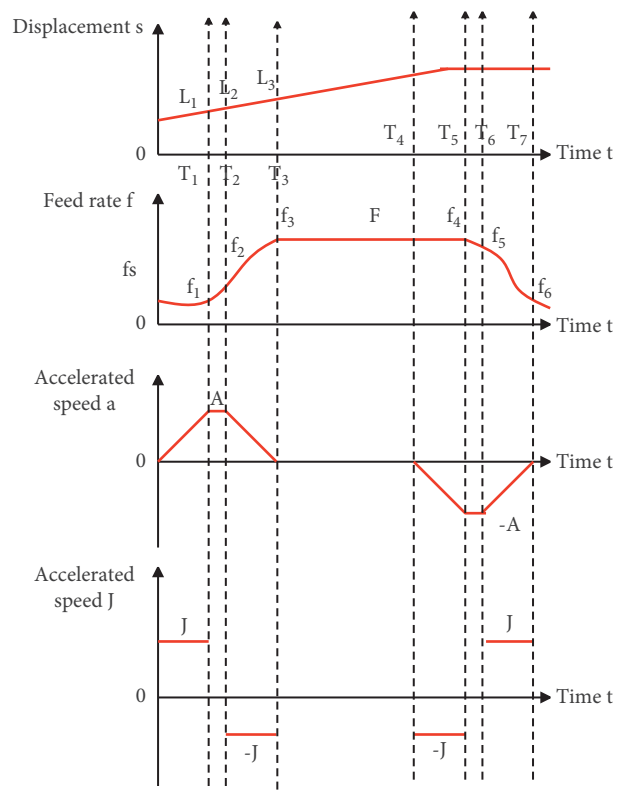

Figure 5: S-type acceleration and deceleration.

$$u_{i+1} = u_i + \frac{T_s v(u_i)}{(\sqrt{dx/du})^2 + (\sqrt{dy/du})^2 + (\sqrt{dz/du})^2}. \tag{32}$$

The above formula is the solution formula of the next interpolation point obtained by the first-order Taylor expansion method.

$$u_{i+1} = u_i + \frac{T_s v(u_i)}{(\sqrt{dx/du})^2 + (\sqrt{dy/du})^2 + (\sqrt{dz/du})^2} + \frac{\left[dx/du + d^2x/du^2 + dy/du + d^2y/du^2 + dz/du + d^2z/dz^2\right]}{2\left[(\sqrt{dx/du})^2 + (\sqrt{dy/du})^2 + (\sqrt{dz/du})^2\right]^2}. \tag{33}$$

The above formula is the solution formula of the next interpolation point obtained by the second-order Taylor expansion method.

The cubic polynomial of arc length and parameter can be expressed as follows: $u = a + bS + cS^2 + dS^3$. The premise of parameter interpolation is to calculate the temporary parameter value, which takes the first-order Taylor interpolation as the starting point.

$$u_{i+1} = u'_{i+1} + \Delta(u_i). \tag{34}$$

Among them, $\Delta(u_i)$ is the compensation value, u'_{i+1} is the temporary parameter value (obtained by the first-order Taylor expansion method), a cubic polynomial is established between the positions $C(u)$ and $C(u'_1 + 1)$, the arc length is the independent variable, and the parameter

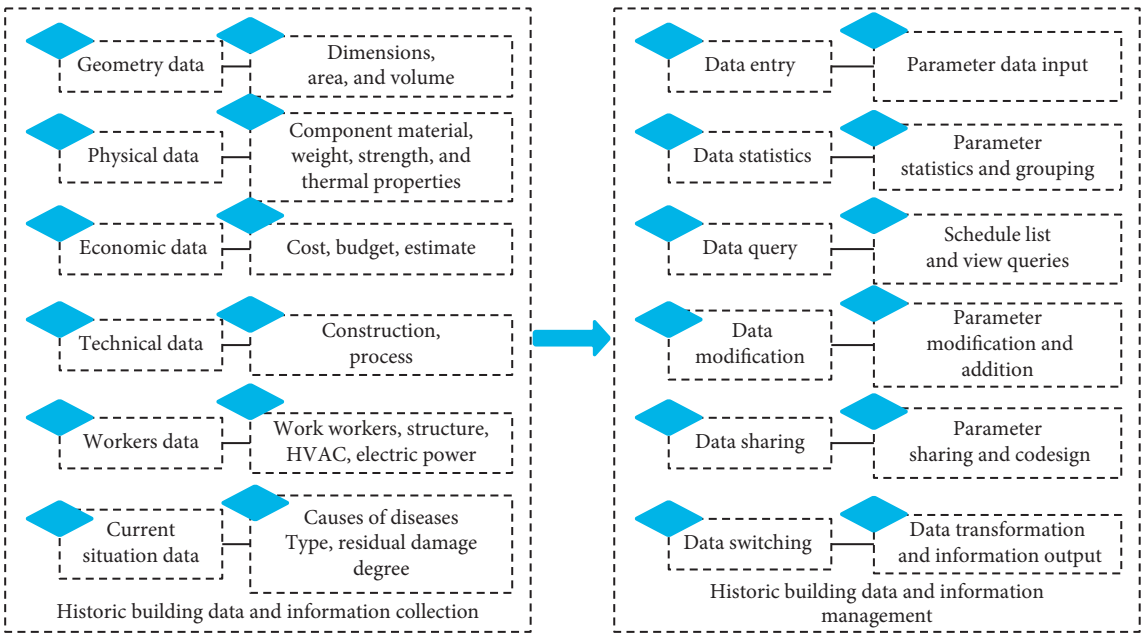

Figure 6: Comprehensive data information of historical buildings.

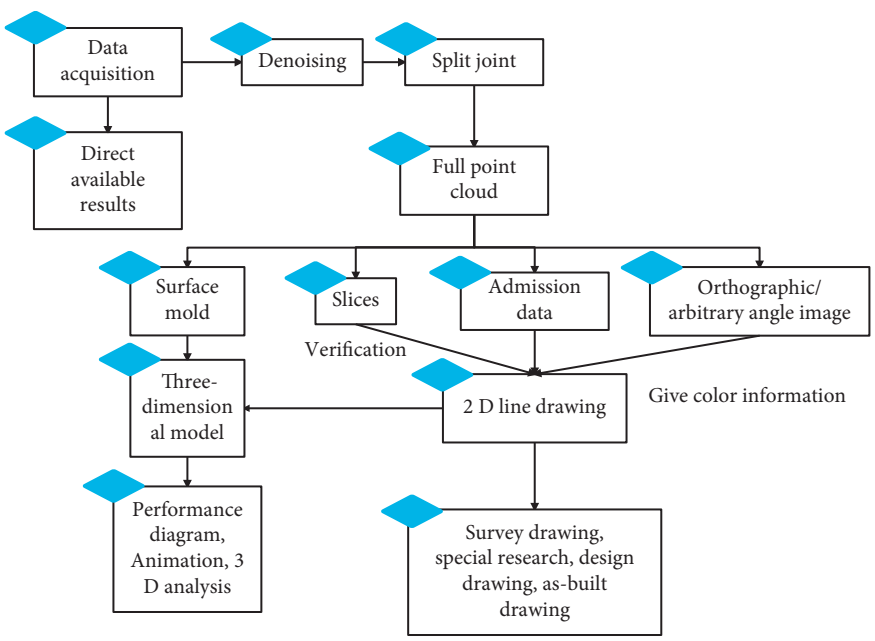

Figure 7: Process of building scanning data collection and utilization.

u is the dependent variable. In this case, the solution is based on a system of equations consisting of two derivatives and two position equations. According to the knowledge of calculus geometry, $u\prime(S) = 1/C\prime(u)$ can be known. In order to simplify the calculation process, the arc length can be replaced by the chord length, that is, $L = \|C(u_i) - C(u_{i+1}')\|$. From this, a cubic polynomial can be established to solve the four parameters a, b, c, and d. The four equations established can be represented by a matrix as follows:

$$\begin{bmatrix} u_i \\ \frac{du}{dL}\Big|_{L=0} \\ u_{i+1}' \\ \frac{du}{dL} \end{bmatrix} = \begin{bmatrix} 0 & 0 & 0 & 1 \\ 0 & 0 & 1 & 0 \\ L^3 & L^2 & L & 1 \\ 3L^2 & 2L & 1 & 0 \end{bmatrix} \begin{bmatrix} a \\ b \\ c \\ d \end{bmatrix}. \tag{35}$$

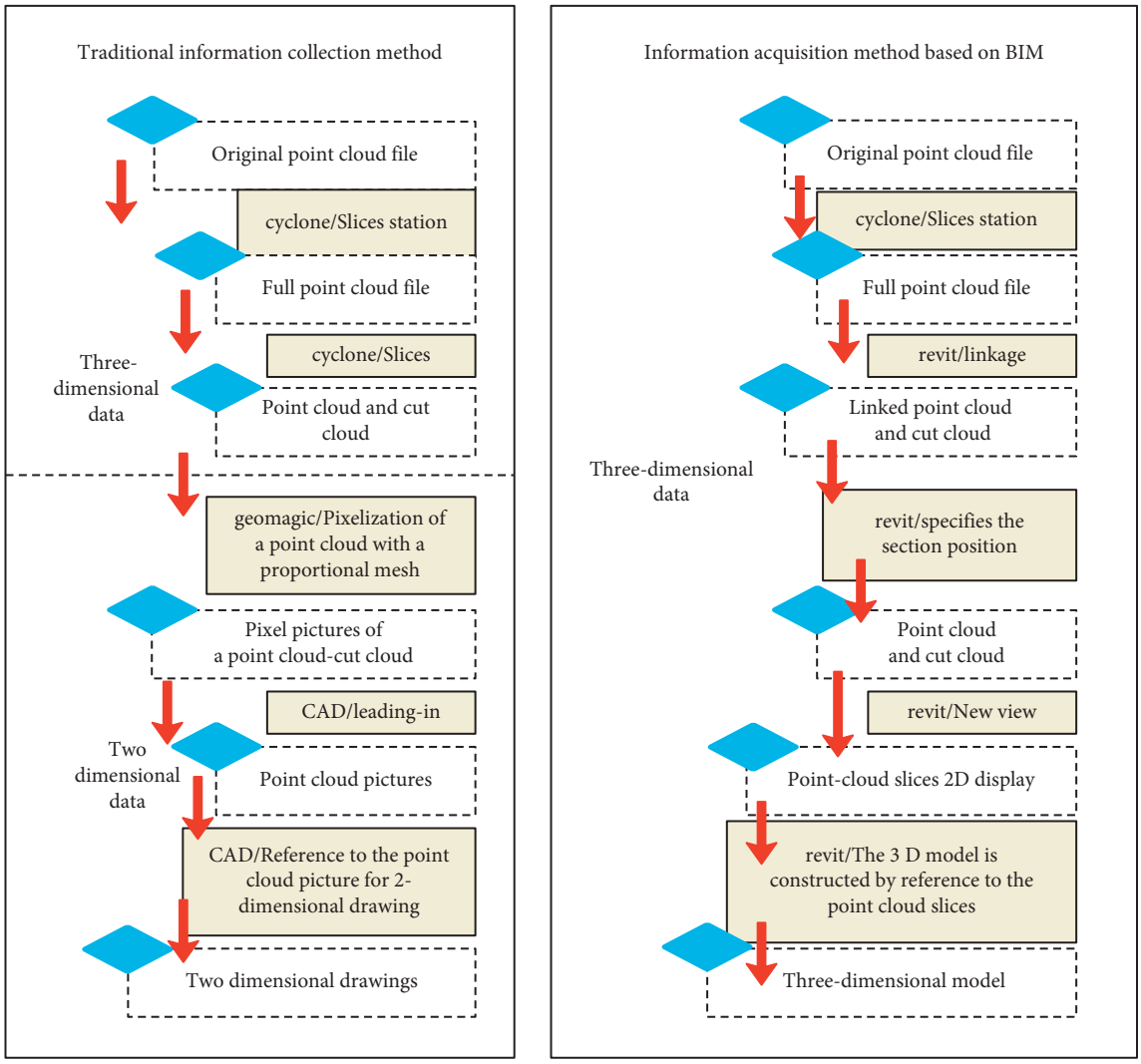

Figure 8: The process of the traditional way and the BIM way of working.

Table 1: Evaluation of building structure construction.

Num	Building structure	Num	Building structure
1	87.51	12	92.04
2	85.96	13	84.71
3	85.23	14	84.56
4	86.31	15	91.30
5	87.51	16	88.64
6	88.05	17	88.72
7	86.98	18	85.42
8	88.93	19	92.61
9	90.70	20	87.81
10	88.76	21	88.01
11	92.77	22	92.44

It can be obtained that the coefficient vector φ has a unique solution $\varphi = \phi^{-1} \cdot \delta$

We assume that the interpolation feed rate is $V(u_i)$, and the displacement in the interpolation period is $s_i = V(\xi)$. The parameter u_{i+1} is calculated as

$$u_{i+1} = a \cdot (S_i)^3 + b \cdot (S_i)^2 + c \cdot (S_i) + d. \tag{36}$$

Combining the above formula, the four coefficients a, b, c, and d can be solved.

$$\begin{cases} a = \dfrac{AL - 2B}{L^3}, \\ b = \dfrac{A}{2L} - \dfrac{3(AL - 2B)}{3L^2} \quad \text{among: } B = \dot{u}_L - \dot{u}_0 A = u_{i+1} - u_i - \dot{u}_0 L, \\ c = \dot{u}_0, \\ d = u_i. \end{cases} \tag{37}$$

The quintic polynomial of the same arc length and parameters can also be solved in the same way.

Table 2: Evaluation of the effect of building information protection methods of urban historical features based on BIM technology.

Num	Building information protection	Num	Building information protection
1	80.66	12	88.73
2	84.14	13	84.76
3	86.68	14	78.99
4	85.07	15	78.29
5	84.78	16	79.98
6	85.95	17	78.94
7	85.72	18	79.04
8	80.03	19	88.58
9	80.65	20	80.05
10	83.32	21	82.69
11	86.31	22	88.37

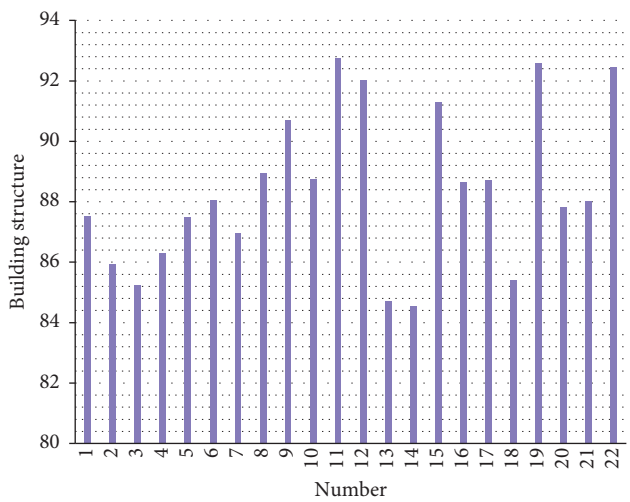

Figure 9: Statistical diagram of the evaluation of building structure construction.

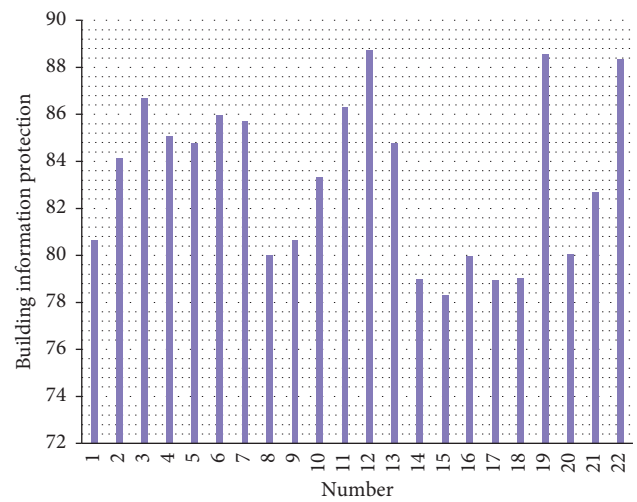

Figure 10: Statistical diagram of the evaluation of the effect of building information protection methods for urban historical features based on BIM technology.

4. Building Information Protection Method of Urban Historical Style Based on BIM Technology

The BIM database does not only refer to geometric figures but also contains any form of information that can be recognized by a computer, including any form of record, description, statistics, and explanation information that can be recognized by a computer. It includes geometric data with dimensional parameters, physical data of building components, cost data of protection and repair, technical data of construction technology and procedures, worker data of related types of work, and status data of building diseases. These data can include geometric data, physical data, economic data, technical data, worker data, and status data (Figure 6). The construction of a historical building database can provide a data storage medium for building protection and repair, information sharing, and interaction. The database of historical buildings includes the geometric database of historical buildings, the database of archives information, and the database of repair and protection schemes.

3D laser scanning technology is a data acquisition and processing technology centered on 3D laser scanning technology and scanning information processing technology. The complete point cloud loses its own integrity in various indirect uses, resulting in increased error opportunities (Figure 7).

Although the existing traditional information collection methods also use 3D laser scanning technology, as described above, the later slicing leads to dimensionality reduction of information, and this 2D use method is not the best way to cooperate with 3D laser scanning. In the working method based on the BIM concept, the point cloud always carries 3D information but can be freely presented in 2D and 3D, and the point cloud file itself has not changed irreversibly. Therefore, the application of point cloud based on the BIM concept avoids the dimensionality reduction of information, which is more advantageous than the traditional method (Figure 8).

On the basis of the above model, the effect evaluation of the building information protection method of urban historical features based on BIM technology is carried out, and the protection effects of building structure construction and

historical features buildings are evaluated, respectively. The results are shown in Tables 1 and 2 and Figures 9 and 10.

The above experimental studies have verified that the building information protection method of urban historical features based on BIM technology has a good effect and can effectively promote the building information protection of urban historical features.

5. Conclusion

Architectural cultural heritage is often built through the careful consideration of craftsmen during the initial construction period, and it has the essence of architectural entities and the essence of space creation. The entire building complex complements its own information expression with the help of the natural space environment, the ontology is well-distributed, and the space environment changes and forms a grand architectural momentum. It is a typical representative of regional architectural features. From such existing urban architectural cultural heritage, we can fully experience the bearing of the space environment on the ontology, and the space environment nourishes the ontology in the historical development. This paper combines BIM technology to study the building information protection method of urban historical features. The experimental study verifies that the building information protection method of urban historical features based on BIM technology has a good effect and can effectively promote the building information protection of urban historical features.

Data Availability

The labeled dataset used to support the findings of this study is available from the corresponding author upon request.

Conflicts of Interest

The authors declare that there are no conflicts of interest.

Acknowledgments

This study was supported by 2021 Hainan Provincial Natural Science Foundation of China "Study on the strategy of cluster protection and reuse of Hainan traditional settlement heritage from the perspective of rural revitalization" (No. 721RC604).

References

[1] S. Ahmed, "Barriers to implementation of building information modeling (BIM) to the construction industry: a review," *Journal of civil engineering and construction*, vol. 7, no. 2, p. 107, 2018.

[2] I. Othman, Y. Y. Al-Ashmori, Y. Rahmawati, Y. H. Mugahed Amran, and M. A. M. Al-Bared, "The level of building information modelling (BIM) implementation in Malaysia," *Ain Shams Engineering Journal*, vol. 12, no. 1, pp. 455–463, 2021.

[3] R.-R. Dong, "The application of BIM technology in building construction quality management and talent training," *Eurasia Journal of Mathematics, Science and Technology Education*, vol. 13, no. 7, pp. 4311–4317, 2017.

[4] X. Qin, Y. Shi, K. Lyu, and Y. Mo, "Using a TAM-TOE model to explore factors of Building Information Modelling (BIM) adoption in the construction industry," *Journal of Civil Engineering and Management*, vol. 26, no. 3, pp. 259–277, 2020.

[5] Y.-C. Kim, W.-H. Hong, J.-W. Park, and G.-W. Cha, "An estimation framework for building information modeling (BIM)-based demolition waste by type," *Waste Management & Research: The Journal for a Sustainable Circular Economy*, vol. 35, no. 12, pp. 1285–1295, 2017.

[6] M. N. Kocakaya, E. Namlı, and Ü. Işıkdağ, "Building information management (BIM), a new approach to project management," *Journal of sustainable construction materials and technologies*, vol. 4, no. 1, pp. 323–332, 2019.

[7] T. Wei and Y. Chen, "Green building design based on BIM and value engineering," *Journal of Ambient Intelligence and Humanized Computing*, vol. 11, no. 9, pp. 3699–3706, 2020.

[8] S. M. Noor, S. R. Junaidi, and M. K. A. Ramly, "Adoption of building information modelling (bim): factors contribution and benefits," *Journal of Information System and Technology Management*, vol. 3, no. 10, pp. 47–63, 2018.

[9] E. Papadonikolaki, C. van Oel, and M. Kagioglou, "Organising and managing boundaries: a structurational view of collaboration with building information modelling (BIM)," *International Journal of Project Management*, vol. 37, no. 3, pp. 378–394, 2019.

[10] Y. Y. Al-Ashmori, I. Othman, Y. Rahmawati et al., "BIM benefits and its influence on the BIM implementation in Malaysia," *Ain Shams Engineering Journal*, vol. 11, no. 4, pp. 1013–1019, 2020.

[11] A. Koutamanis, J. Heuer, and K. D. Könings, "A visual information tool for user participation during the lifecycle of school building design: BIM," *European Journal of Education*, vol. 52, no. 3, pp. 295–305, 2017.

[12] S.-M. Luo, J. Xu, and B.-K. Li, "Practice and exploration on teaching reform of engineering project management course in universities based on BIM simulation technology," *Eurasia Journal of Mathematics, Science and Technology Education*, vol. 14, no. 5, pp. 1827–1835, 2018.

[13] C.-J. Chen, S.-y. Chen, S.-h. Li, and H.-t. Chiu, "Green BIM-based building energy performance analysis," *Computer-Aided Design and Applications*, vol. 14, no. 5, pp. 650–660, 2017.

[14] H. R. Abed, W. A. Hatem, and N. A. Jasim, "Adopting BIM technology in fall prevention plans," *Civil Engineering Journal*, vol. 5, no. 10, pp. 2270–2281, 2019.

[15] L. Joblot, T. Paviot, D. Deneux, and S. Lamouri, "Literature review of Building Information Modeling (BIM) intended for the purpose of renovation projects," *IFAC-PapersOnLine*, vol. 50, no. 1, pp. 10518–10525, 2017.

[16] P. Wu, R. Jin, Y. Xu, F. Lin, Y. Dong, and Z. Pan, "The analysis of barriers to bim implementation for industrialized building construction: a China study," *Journal of Civil Engineering and Management*, vol. 27, no. 1, pp. 1–13, 2021.

[17] A. Ahankoob, K. Manley, C. Hon, and R. Drogemuller, "The impact of building information modelling (BIM) maturity and experience on contractor absorptive capacity," *Architectural Engineering and Design Management*, vol. 14, no. 5, pp. 363–380, 2018.

[18] M. Deng, C. C. Menassa, and V. R. Kamat, "From BIM to digital twins: a systematic review of the evolution of intelligent building representations in the AEC-FM industry," *Journal of Information Technology in Construction*, vol. 26, no. 5, pp. 58–83, 2021.